Measurements of Thermal Rate Constants and Theoretical Calculations for the N(^{2}D, ^{2}P) + C_2H_2 and C_2D_2 Reactions

Toshiyuki Takayanagi* and Yuzuru Kurosaki

Advanced Science Research Center, Japan Atomic Energy Research Institute, Tokai-mura, Naka-gun, Ibaraki 319-1195, Japan

Kazuaki Misawa, Madoka Sugiura, Yasuhide Kobayashi, Kei Sato, and Shigeru Tsunashima

Department of Applied Physics, Tokyo Institute of Technology, Ookayama, Meguro-ku, Tokyo 152-8551, Japan

Received: February 17, 1998; In Final Form: April 16, 1998

Rate constants for the reactions N(^{2}D,^{2}P) + C_2H_2 and C_2D_2 have been measured using a technique of pulse radiolysis−resonance absorption between 220 and 293 K. Arrhenius parameters have been determined from the temperature dependence of the measured rate constants; the activation energies for the reactions of N(^{2}D) were about 0.5 kcal/mol, while those for N(^{2}P) were about 0.9 kcal/mol. The H/D isotope effect was found to be very small for both the N(^{2}D) + C_2H_2 and N(^{2}P) + C_2H_2 reactions. The rate constants for N(^{2}D) + C_2H_2 were found to be about 3 times as large as those for N(^{2}P) + C_2H_2. To understand the overall reaction mechanism of the N(^{2}D) + C_2H_2 reaction, ab initio molecular orbital calculations of the lowest doublet potential energy surface have been performed. It has been found that the initial step of the reaction is the addition of the N atom to the π bond of acetylene. The rate constants have been calculated using conventional transition-state theory and compared to the experimental results. Possible reaction pathways are discussed on the basis of the ab initio results.

1. Introduction

The reactivity of the N atom in the electronic ground state or excited state has long been of great interest since the reactions of N with hydrocarbon molecules are important in various fields including interstellar chemistry, combustion chemistry, and atmospheric chemistry.[1] Despite its importance, there have been much fewer studies on the reactions of the N atom in contrast to the extensive studies on the reactions of other atoms such as an O(^{3}P, ^{1}D) atom. In particular, the detailed mechanism and dynamics for the reactions of N atoms with hydrocarbon molecules have not been understood well since the initial reaction products have not directly been detected yet; most of the reaction mechanisms have been speculated on the basis of final products analysis. Very recently, however, Umemoto et al.[2,3] have employed two-photon photolysis of NO to produce N(^{2}D) and studied the reactions of N(^{2}D) with saturated hydrocarbon molecules such as CH_4, C_2H_6, and C_3H_8. They succeeded in determining the initial rovibrational distributions of the NH molecule produced in the reactions.[2,3] In the near future, this technique will be applied to other molecules. In addition to advances in experimental techniques, ab initio molecular orbital calculations have been becoming more quantitative and very useful to understand the reaction mechanisms of N atoms.[4,5]

In this paper we study the reactions of N atoms with acetylene. Although the reactions of N atoms with C_2H_2 are expected to be simple, information on the reaction mechanism and dynamics is still insufficient. Safrany and co-workers[1,6] extensively studied the reaction of so-called "active nitrogen" with various hydrocarbon molecules using a technique of mass spectroscopy. They suggested that the main exit channel for the N + C_2H_2 reaction is HCCN + H; however, the electronic state of the N atom was not identified. Measurements of the rate constants are also available. The rate constant for the N(^{4}S) + C_2H_2 reaction has been reported to be very small ($\sim 10^{-16}$ cm^3 molecule^{-1} s^{-1}) at room temperature,[7,8] while the rate constant for the N(^{2}D) + C_2H_2 reaction has been determined to be 1.1×10^{-10} cm^3 molecule^{-1} s^{-1} at room temperature.[9] The rate constant for the N(^{2}P) + C_2H_2 reaction has also been measured to be 2.3×10^{-11} cm^3 molecule^{-1} s^{-1} in our laboratory.[10] There have been no reports on the temperature dependence of the rate constants for these reactions

Very recently, Casavecchia and co-workers[11] have carried out crossed molecular beam measurements of product angular and velocity distributions for the N(^{2}D) + C_2H_2 reaction. They directly detected the HCCN radical as a primary product of the reaction and found that the reaction proceeds through a long-lived complex. Although detailed experimental data have not been published yet, these results would significantly contribute to further understanding of the reaction mechanism and dynamics.

In this paper, we present the experimental results for the temperature dependence of the rate constants for the reactions of the N(^{2}D) and N(^{2}P) atoms with C_2H_2 using a pulse radiolysis−resonance absorption technique since a knowledge of the activation energies generally gives important information on the potential energy surfaces. This experimental technique was previously applied to the N(^{2}D, ^{2}P) + H_2 system.[12] The H/D isotope effect was also examined by using C_2D_2. In addition, we present ab initio molecular orbital calculations of the transition states and reaction pathways for the N(^{2}D) + C_2H_2 reaction in order to understand overall reaction mechanisms. Conventional transition-state theory calculations of the rate

* Corresponding author. E-mail address: tako@popsvr.tokai.jaeri.go.jp.

S1089-5639(98)01163-3 CCC: $15.00
Published on Web 07/10/1998

constants were also carried out using the ab initio results and compared to the experimental results.

2. Experimental Section

The experimental apparatus and procedure were very similar to those described previously.[12] A mixture of N_2 and C_2H_2 (C_2D_2) in a stainless steel vessel was irradiated by a pulsed electron beam from a Febetron 706 apparatus (Hewlett-Packard) to produce $N(^2D)$ and $N(^2P)$. The time profile of the concentration of $N(^2D)$ and $N(^2P)$ was monitored using the absorption of atomic lines at 149 and 174 nm, respectively. These atomic lines were derived from a CW microwave discharge in a flow of N_2/He. Transmitted light was detected with a photomultiplier tube (Hamamatsu, R976) through a VUV monochromator (Shimadzu, SGV-50). The signal was amplified and processed with a wave memory (NF Circuit Design Block, WM-852) and a personal computer (NEC, PC-9801F). Since the fine structures of the atomic lines were not able to be resolved in the present experimental system, the rate constant obtained is averaged over spin−orbit sublevels. For the measurement of $N(^2P)$, the typical pressure of N_2 was kept at 700 Torr, while the C_2H_2 (C_2D_2) pressure was varied between 0 and 20 mTorr. For the measurement of $N(^2D)$, the gas mixture was diluted with He because $N(^2D)$ is deactivated efficiently by N_2.[12] Typical pressures of C_2H_2 (C_2D_2), N_2, and He were 0−10 mTorr, 1 Torr, and 700 Torr, respectively. The yield of $N(^2P)$ must be much smaller than that of $N(^2D)$. C_2D_2 was synthesized from calcium carbide and deuterium oxide. The isotopic purity was larger than 95%. N_2 (Nihon Sanso), He (Japan Helium Center), and C_2H_2 (Takachiho Shoji) are purified by usual methods.

3. Method of ab Initio Molecular Orbital Calculations

All ab initio calculations were performed with the GAUSSIAN 94 system.[13] Geometry optimizations for various stationary points were carried out at the MP2(full) level of theory using the correlation consistent polarized valence triple-ζ (cc-pVTZ) basis set of Dunning.[14] Harmonic vibrational frequencies were calculated at the same level of theory. The final energy diagram was obtained from the MP4(full,SDTQ)/cc-pVTZ calculations, in which the spin projection method was applied in order to remove the spin contamination from unwanted spin states (denoted here by PMP4).[4,5] The transition-state geometry for the addition reaction of $N(^2D)$ to C_2H_2 was, on the other hand, optimized at the complete active space self-consistent-field (CASSCF) level of theory with the cc-pVTZ basis set because single-reference Hartree−Fock theory cannot be applied in an early region of the potential energy surface of $N(^2D) + C_2H_2$. The active space employed includes seven orbitals: three nitrogen *2*p orbitals, two CC π, and two CC π^* orbitals of C_2H_2. Seven electrons were distributed among these orbitals.

4. Results and Discussion

A. Experimental Rate Constants. The time dependence of the concentration of $N(^2D)$ and $N(^2P)$ was fitted to the pseudo-first-order decay. Figure 1 shows a typical plot of the decay rates of $N(^2D)$ as a function of C_2H_2 pressure at 273 K. The rate constant for each temperature can be obtained from the slope of the corresponding linear plot. Similar plots were obtained for other systems: $N(^2D) + C_2D_2$, $N(^2P) + C_2H_2$, and $N(^2P) + C_2D_2$. Table 1 summarizes the measured rate constants; the error limit is one standard deviation. Our rate constants are also compared to other values in Table 1. The rate constant for $N(^2D) + C_2H_2$ at 300 K was previously measured to be 1.1×10^{-10} cm^3 molecule^{-1} s^{-1} by Fell et al.[9] using a technique of electron spin resonance (ESR) absorption. It is seen that their value is larger than our value (6.7×10^{-11} cm^3 molecule^{-1} s^{-1}) at 293 K by a factor of about 2. As mentioned in the Introduction, we previously measured the rate constant for the $N(^2D) + H_2$ reaction using the present experimental technique and found that our results at room temperature were in satisfactory agreement with that measured by Fell et al.[12] Therefore, it is very difficult to understand the main source of this disagreement for $N(^2D) + C_2H_2$. The rate constant for $N(^2P) + C_2H_2$ at 295 K was previously measured to be 2.3×10^{-12} in our laboratory,[10] which is in excellent agreement with the present value at 293 K, as shown in Table 1.

The temperature dependence of the rate constants is found to be well reproduced by the standard Arrhenius equation, as shown in Figure 2. The Arrhenius parameters calculated by a nonlinear least-squares method are listed in Table 2.

Two conclusions can be derived from the present experimental results. First, the H/D isotope effect is very small for

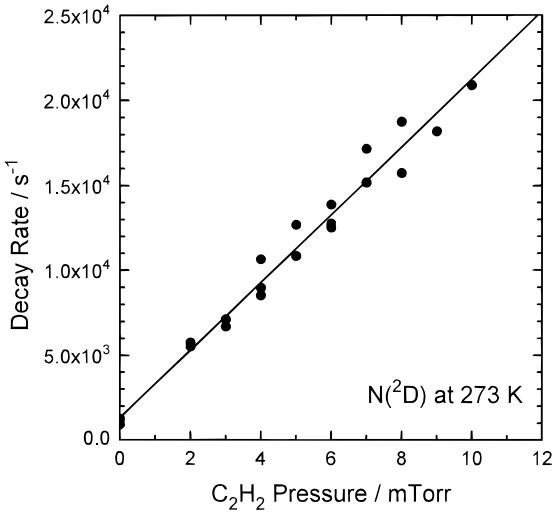

Figure 1. Typical plot of the pseudo-first-order decay rate of $N(^2D)$ as a function of C_2H_2 pressure at 273 K.

TABLE 1: Rate Constants for the Reactions of $N(^2D)$ and $N(^2P)$ with C_2H_2 and C_2D_2

reaction	T/K	k/cm^3 molecule^{-1} s^{-1}
	Present Work	
$N(^2D) + C_2H_2$	293	$(6.7 \pm 0.3) \times 10^{-11}$
	273	$(6.1 \pm 0.2) \times 10^{-11}$
	253	$(5.5 \pm 0.4) \times 10^{-11}$
	233	$(5.3 \pm 0.2) \times 10^{-11}$
	223	$(4.9 \pm 0.2) \times 10^{-11}$
$N(^2D) + C_2D_2$	293	$(6.3 \pm 0.2) \times 10^{-11}$
	273	$(5.9 \pm 0.3) \times 10^{-11}$
	253	$(5.5 \pm 0.2) \times 10^{-11}$
	233	$(5.2 \pm 0.2) \times 10^{-11}$
	223	$(4.8 \pm 0.2) \times 10^{-11}$
$N(^2P) + C_2H_2$	293	$(2.2 \pm 0.1) \times 10^{-11}$
	273	$(2.0 \pm 0.1) \times 10^{-11}$
	253	$(1.8 \pm 0.1) \times 10^{-11}$
	233	$(1.5 \pm 0.1) \times 10^{-11}$
	223	$(1.3 \pm 0.1) \times 10^{-11}$
$N(^2P) + C_2D_2$	293	$(2.0 \pm 0.1) \times 10^{-11}$
	270	$(1.7 \pm 0.1) \times 10^{-11}$
	250	$(1.5 \pm 0.1) \times 10^{-11}$
	233	$(1.4 \pm 0.1) \times 10^{-11}$
	220	$(1.3 \pm 0.1) \times 10^{-11}$
	Literature Values	
$N(^2D) + C_2H_2$	300	$(11.4 \pm 3.5) \times 10^{-11}$[a]
$N(^2P) + C_2H_2$	295	$(2.3 \pm 0.2) \times 10^{-11}$[b]

[a] Ref 9. [b] Ref 10.

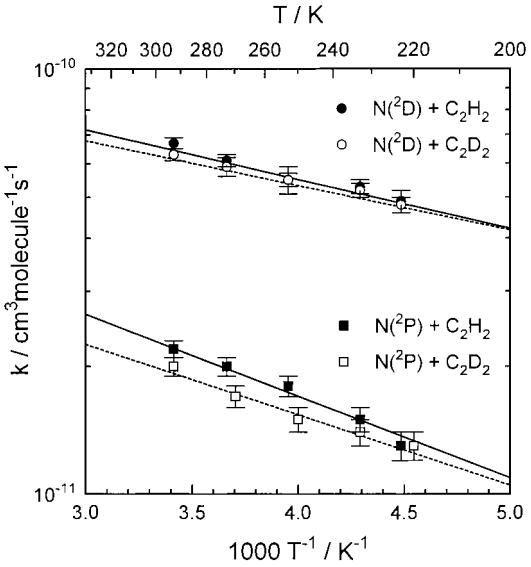

Figure 2. Arrhenius plots of the rate constants for N(^{2}D) + C_2H_2 (solid circles), N(^{2}D) + C_2D_2 (open circles), N(^{2}P) + C_2H_2 (solid squares), and N(^{2}P) + C_2D_2 (open squares). The lines indicate Arrhenius fits to the experimental data.

TABLE 2: Arrhenius Parameters for the Reactions of N(^{2}D) and N(^{2}P) with C_2H_2 and C_2D_2

reaction	A/cm^3 molecule^{-1} s^{-1}	E_a/kcal/mol
N(^{2}D) + C_2H_2	$(1.6 \pm 0.2) \times 10^{-10}$	0.53 ± 0.06
N(^{2}D) + C_2D_2	$(1.4 \pm 0.1) \times 10^{-10}$	0.48 ± 0.05
N(^{2}P) + C_2H_2	$(1.0 \pm 0.1) \times 10^{-10}$	0.88 ± 0.06
N(^{2}P) + C_2D_2	$(0.71 \pm 0.12) \times 10^{-10}$	0.76 ± 0.09

both the N(^{2}D) + C_2H_2 and N(^{2}P) + C_2H_2 reactions. This result strongly suggests that the difference in the barrier heights between N(^{2}D, ^{2}P) + C_2H_2 and N(^{2}D,^{2}P) + C_2D_2 is very small and that both the reactions have an early transition state. Second, the rate constants for N(^{2}D) + C_2H_2 are larger than those for N(^{2}P) + C_2H_2 by a factor of about 3.

The difference in the reactivity between N(^{2}D) and N(^{2}P) with various molecules was previously discussed by Umemoto et al.[10] For saturated hydrocarbons such as CH_4, the rate constants for N(^{2}D) are much larger than those for N(^{2}P) without exception despite the fact that the N(^{2}P) atom has a larger electronic energy. For example, the ratios of the rate constants have been reported to be 60 for CH_4 and 50 for C_2H_6. They suggested that the deactivation mechanism of N(^{2}D) by saturated hydrocarbon molecules is a chemical reaction on the basis of the simple adiabatic electronic energy correlation concept.[10] If we apply this concept to the present N(^{2}D) + C_2H_2 system, for example, the lowest doublet potential energy surface for this system should adiabatically correlate to that for a stable radical such as HCCNH(^{2}A″). Therefore, it is expected that the primary products of the N(^{2}D) + C_2H_2 reaction may be unimolecular decomposition products of this radical, if the collision complex is formed. Also, the potential surface of N(^{2}D) + C_2H_2 adiabatically correlates to that of NH($^3\Sigma$) + CH($^2\Sigma$) under C_s symmetry. Thus, it is reasonable that the deactivation process of N(^{2}D) mainly includes chemical reactions. The possible reaction pathways will be further discussed using ab initio molecular orbital calculations in the following section. In contrast to the exit channels of the reactions of N(^{2}D), on the other hand, Umemoto et al. suggested that the N(^{2}P) atom is deactivated to N(^{2}D) or N(^{4}S) via nonadiabatic transition by the collision with saturated hydrocarbon molecules, since the deactivation rate constants for N(^{2}P) are smaller than those for

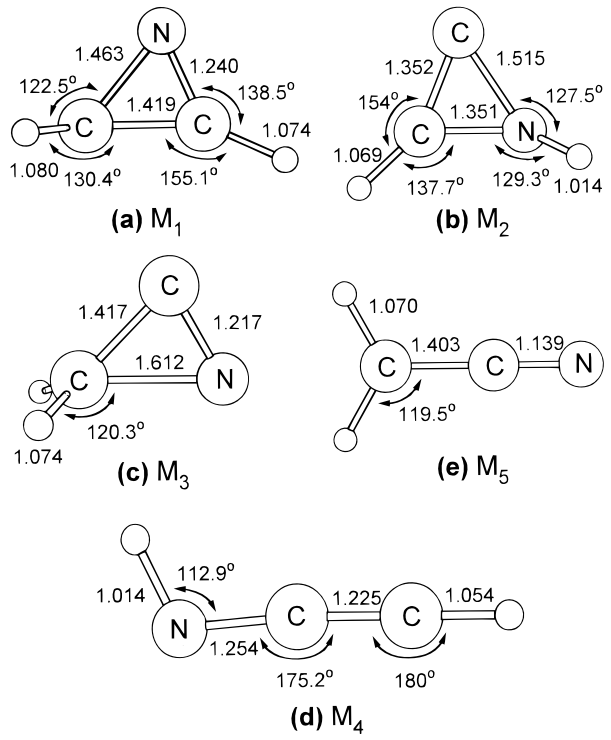

Figure 3. Molecular geometries of the stationary points (minima) on the potential energy surface of the N(^{2}D) + C_2H_2 reaction: (a) M_1, (b) M_2, (c) M_3, (d) M_4, and (e) M_5. All the geometrical parameters were calculated at the MP2(full)/cc-pVTZ level of theory (bond lengths in angstroms, angles in degrees).

N(^{2}D).[10] In the case of unsaturated hydrocarbon molecules, however, the difference in the reactivity between N(^{2}D) and N(^{2}P) is not clear compared to the case of saturated hydrocarbons. For example, the rate constants for N(^{2}D) + C_2H_4 and for N(^{2}P) + C_2H_4 have been measured to be almost comparable,[9,10] while the ratio of the rate constants between N(^{2}D) + CH_2═CF_2 and N(^{2}P) + CH_2═CF_2 is reported to be about 8.[9,10] Since the present experimental results indicate that the ratio of the rate constants of N(^{2}D) + C_2H_2 and N(^{2}P) + C_2H_2 reactions are about 3, the mechanism of the deactivation process of N(^{2}P) would presumably be similar to the N(^{2}P) + CH_2═CF_2 case. One of the possible deactivation mechanisms of N(^{2}P) by C_2H_2 is electronic energy transfer to the triplet state of C_2H_2 as N(^{2}P) + $C_2H_2(^1\Sigma) \rightarrow$ N(^{4}S) + $C_2H_2(^3B_2)$. This process can be exothermic if the energy separation between the triplet and singlet states of the C_2H_2 molecule is smaller than 82 kcal/mol, which corresponds to the energy difference between N(^{2}P) and N(^{4}S). The energy difference between the singlet and triplet states of C_2H_2 has not been experimentally determined yet, although Bowman and Miller[15] tentatively assigned this difference to be 46 kcal/mol for their energy loss spectrum. However, previous ab initio molecular orbital calculations[16,17] show that the energy difference between the singlet and triplet states of C_2H_2 is 80−89 kcal/mol depending on the basis set employed and do not strongly support the existence of this energy-transfer process. The possibility of chemical reaction channels cannot be ruled out since the initial products of N(^{2}P) + C_2H_2 have not been directly detected in the present experiment. Further experimental studies as well as theoretical studies of the potential energy surfaces of excited states would definitely be necessary for quantitative understanding of the deactivation processes of the N(^{2}P) atom.

B. Results of ab Initio Calculations. Figures 3 and 4 show the optimized geometries for the various stationary points on

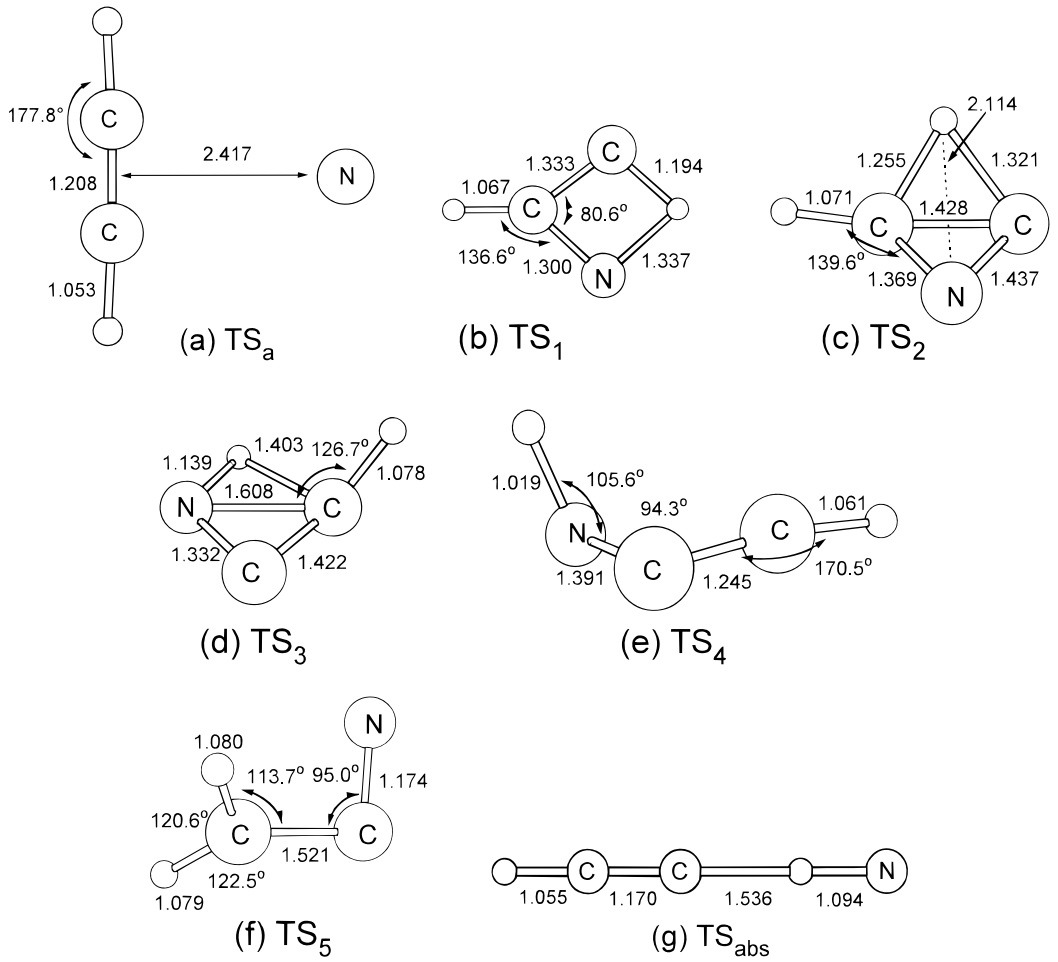

Figure 4. Molecular geometries of the stationary points (transition state) on the potential energy surface of the N(^{2}D) + C_2H_2 reaction: (a) TS_a (b) TS_1, (c) TS_2, (d) TS_3, (e) TS_4, (f) TS_5, and (g) TS_{abs}.

the lowest doublet potential energy surface for the N(^{2}D) + C_2H_2 reaction. Harmonic vibrational frequencies and total energies for these stationary points are summarized in Tables 3 and 4. The relative energies calculated from the PMP4 results are schematically shown in Figure 5. At the PMP4(full,SDTQ)/cc-pVTZ level of theory, the errors in the relative energies may be as large as ±10 kcal/mol. All the intermediate radicals and transition states are denoted as M_i (i = 1−5) and TS_i(i = a, 1−5), respectively.

The present ab initio calculations show that the addition of N(^{2}D) to the π bond of the C_2H_2 molecule is the lowest reaction pathway and produces a stable three-membered radical, M_1, via transition state, TS_a. As shown in Figure 4, the internuclear distance between the N atom and C_2H_2 molecule at the transition state of this addition reaction is calculated to be very long at the CASSCF(7,7)/cc-pVTZ level. In addition, the change in the vibrational frequencies as well as the geometry between the reactant C_2H_2 and the transition state is not so large. These results indicate that the addition reaction of N(^{2}D) to C_2H_2 is classified to have an early transition state. This is also consistent with the present experimental results in which the H/D isotope effect is very small, as mentioned previously. The barrier height including zero-point vibrational energy correction was calculated to be 2.9 kcal/mol at the PMP4(full,SDTQ)/cc-pVTZ level of theory using the CASSCF geometry. This calculated barrier height seems to be too large since the rate constant for N(^{2}D) + C_2H_2 is on the order of $\sim 10^{-10}$ cm^3 molecule^{-1} s^{-1} and the activation energy observed is about 0.5 kcal/mol. This will be further discussed using transition-state theory calculations in the following section. The barrier height calculated at the CASSCF(7,7)/cc-pVTZ level was 5.6 kcal/mol with zero-point vibrational energy correction.

We have also found the transition state for the direct abstraction reaction (TS_{abs}), N(^{2}D) + C_2H_2 → NH($^3\Sigma$) + C$_2$H($^2\Sigma$). The geometry of TS_{abs} was calculated to be linear, as shown in Figure 4. The barrier height for the abstraction reaction was calculated to be 11.1 kcal/mol at the PMP4(full,SDTQ)/cc-pVTZ level of theory with zero-point vibrational energy correction, which is much larger than the barrier height for the addition reaction. This means that we can safely ignore the contribution of the abstraction reaction pathway to overall rate constants.

The intermediate radical, M_1, can isomerize into a ring-opened HNCCH (M_4) radical or CH_2CN (M_5) via corresponding transition states (TS_1−TS_5). Although the CH_2CN radical is the most stable intermediate radical on the potential energy surface, the reaction pathway to produce the HNCCH (M_4) radical via TS_1 and TS_4 is energetically lower than that to produce CH_2CN via TS_3 and TS_5. These two radicals, M_4 and M_5, can dissociate into the lowest product channel, H(^{2}S) + NCCH(^{3}A″). As mentioned in the Introduction, Casavecchia and co-workers[11] have found that the dominant product channel of the N(^{2}D) + C_2H_2 reaction is NCCH + H and that the NCCH radical is produced via a long-lived complex mechanism. The present computational results are qualitatively consistent with their experimental results.

The product channel CH + HCN is calculated to be the second lowest channel; however, we failed to find any transition

TABLE 3: Harmonic Vibrational Frequencies Calculated at MP2(full)/cc-pVTZ

molecule	vibrational frequencies
fragment	
$NH(^3\Sigma)$	3415 (3282)[a]
$CH(^2\Pi)$	2970 (2859)
$CN(^2\Sigma)$	2908 (2069)
$CCH(^2\Sigma)$	822, 822, 2535, 3593
$HCN(^1\Sigma)$	729 (712), 729 (712), 2045 (2097), 3489 (3311)
$HNC(^1\Sigma)$	559 (463), 559 (463), 2048 (2024), 3867 (3653)
$C_2H_2(^1\Sigma)$	600 (612), 600 (612), 759 (730), 759 (730), 1991 (1974), 3445 (3289), 3561(3374)
$C_2H_2(^1\Sigma)$[b]	531 (612), 531 (612), 664 (730), 664 (730), 2065 (1974), 3556 (3289), 3649(3374)
$C_2D_2(^1\Sigma)$	500 (505), 500 (505), 557 (537), 557 (537), 1783 (1762), 2529 (2439), 2812 (2701)
$C_2D_2(^1\Sigma)$[b]	443 (505), 443 (505), 487 (537), 487 (537), 1847 (1762), 2611 (2439), 2886 (2701)
$HNCC(^3A'')$	409, 463, 600, 1153, 2067, 3762
$HCCN(^3A'')$	444 (369), 534 (458), 803, 1082 (1179), 2302 (1735), 3384 (3229)
minimum	
M_1	631, 923, 954, 1068, 1106, 1289, 2077, 3158, 3302
M_2	656, 782, 858, 990, 1017, 1361, 1623, 3349, 3484
M_3	597, 610, 984, 1097, 1165, 1523, 2189, 3207, 3309
M_4	475, 528, 544, 639, 1063, 1286, 1939, 3537, 3575
M_5	416, 483, 631, 1026, 1078, 1484, 2728, 3269, 3376
transition state	
TS_a ($N(^2D) + C_2H_2$)[b]	375i, 162, 533, 535, 667, 675, 2011, 3558, 3644
TS_a ($N(^2D) + C_2D_2$)[b]	375i, 146, 433, 443, 489, 490, 1810, 2613, 2864
TS_1	594i, 694, 799, 1108, 1131, 1668, 2434, 2718, 3380
TS_2	1175i, 729, 839, 893, 1145, 1175, 1472, 2192, 3323
TS_3	844i, 752, 834, 877, 914, 1120, 1484, 2512, 3226
TS_4	611i, 436, 679, 1011, 1125, 1241, 2048, 3471, 3488
TS_5	633i, 200, 694, 961, 1059, 1458, 2274, 3227, 3370
TS_{abs}	809i, 111, 111, 397, 397, 876, 876, 1312, 2593, 3592
$N(^4S) + C_2H_2$	
^4M	480, 666, 907, 912, 1154, 1275, 1314, 3096, 3343
^4TS	1029i, 354, 608, 823, 932, 952, 2036, 3401, 3545

[a] Experimental frequencies in parentheses (refs 19 and 20). [b] Calculated at the CASSCF(7,7)/cc-pVTZ level of theory.

states directly leading to the CH + HCN channel from the intermediate radicals, M_1-M_5. Instead, the HNCCH (M_4) radical can directly dissociate into the CH + HNC channel. According to recent highly accurate ab initio calculations,[18] the barrier height for the isomerization reaction from HNC to HCN is determined to be 33.5 kcal/mol. If we apply this value to the present system, the energy level of the transition state from HNC to HCN becomes larger than the initial energy of $N(^2D) + C_2H_2$. This indicates that the HCN molecule may not be a primary product of the $N(^2D) + C_2H_2$ reaction.

Although an extensive search was made to locate the transition state for the insertion reaction of $N(^2D)$ into the CH bond, $N(^2D) + C_2H_2 \rightarrow$ HNCCH, unfortunately we could not find it. To examine the possibility of the insertion reaction, the interaction potential between $N(^2D)$ and C_2H_2 was calculated at the CASSCF(7,7)/cc-pVTZ level of theory as functions of both the distance (between N and the midpoint of CC) and the orientation angle. The geometry of C_2H_2 was kept in the reactant geometry. The result is plotted in Figure 6. It can be seen that the C_{2v} approach is energetically most favorable. On the other hand, it is found that the collinear approach gives a strongly repulsive interaction. This result is qualitatively consistent with the fact that the transition state for the direct abstraction reaction (TS_{abs}) has a late structure. As shown in Figure 4, the CH distance of TS_{abs} is much larger than the equilibrium CH distance in C_2H_2. This is the reason why the barrier height for abstraction is much larger than that for addition. Similarly, it is suggested that the barrier height for insertion into the CH bond would also be larger than that for addition, because a significant geometry change in C_2H_2 would be necessary at the transition state for insertion. Therefore, it can be concluded that the lowest reaction pathway is the addition of $N(^2D)$ to C_2H_2 and the contribution of abstraction and insertion to the overall rate constants should be small.

TABLE 4: Total Energies and Symmetry for the Reaction $N + C_2H_2 \rightarrow$ Products[a]

	MP2	PMP4	$\langle S^2 \rangle$[b]	symmetry
fragment				
$N(^4S)$	−54.506 81	−54.524 47	3.756	
$N(^2D)$	−54.443 90	−54.436 59	1.766	
$H(^2S)$	−0.499 81	−0.499 81	0.750	
$NH(^3\Sigma)$	−55.129 73	−55.152 32	2.015	$C_{\infty v}$
$CH(^2\Pi)$	−38.393 60	−38.418 86	0.759	$C_{\infty v}$
$CN(^2\Sigma)$	−92.541 33	−92.582 94	0.993	$C_{\infty v}$
$CCH(^2\Sigma)$	−76.499 29	−76.493 33	1.016	$C_{\infty v}$
$HCN(^1\Sigma)$	−93.281 16	−93.307 89	0.000	$C_{\infty v}$
$HNC(^1\Sigma)$	−93.252 17	−93.282 15	0.000	$C_{\infty v}$
$C_2H_2(^1\Sigma)$	−77.188 69	−77.219 94	0.000	$D_{\infty h}$
$HNCC(^3A'')$	−131.124 14	−131.176 75	2.104	C_s
$HCCN(^3A'')$	−131.170 35	−131.230 23	2.249	C_s
minimum				
M_1	−131.769 88	−131.819 69	0.832	C_1
M_2	−131.734 07	−131.781 86	0.774	C_1
M_3	−131.780 98	−131.830 26	0.807	C_s
M_4	−131.799 36	−131.858 35	0.910	C_s
M_5	−133.855 53	−131.911 43	0.881	C_{2v}
transition state				
TS_a[c]		−131.651 98		C_{2v}
TS_1	−131.710 15	−131.768 73	0.908	C_s
TS_2	−131.695 35	−131.726 69	0.780	C_1
TS_3	−131.678 78	−131.732 44	0.832	C_1
TS_4	−131.694 26	−131.756 87	1.000	C_1
TS_5	−131.760 15	−131.821 70	0.954	C_1
TS_{abs}	−131.568 86	−131.635 61	2.023	$D_{\infty h}$
$N(^4S) + C_2H_2$				
^4M	−131.709 33	−131.772 92	4.009	C_s
^4TS	−131.647 25	−131.713 84	4.048	C_s

[a] All the geometries except for TS_a were optimized at the MP2(full)/cc-pVTZ level of theory. [b] Calculated at the HF/cc-pVTZ//MP2(full)/cc-pVTZ level of theory. [c] Calculated at the PMP4(full,STDQ)/cc-pVTZ//CASSCF(7,7)/cc-pVTZ level of theory.

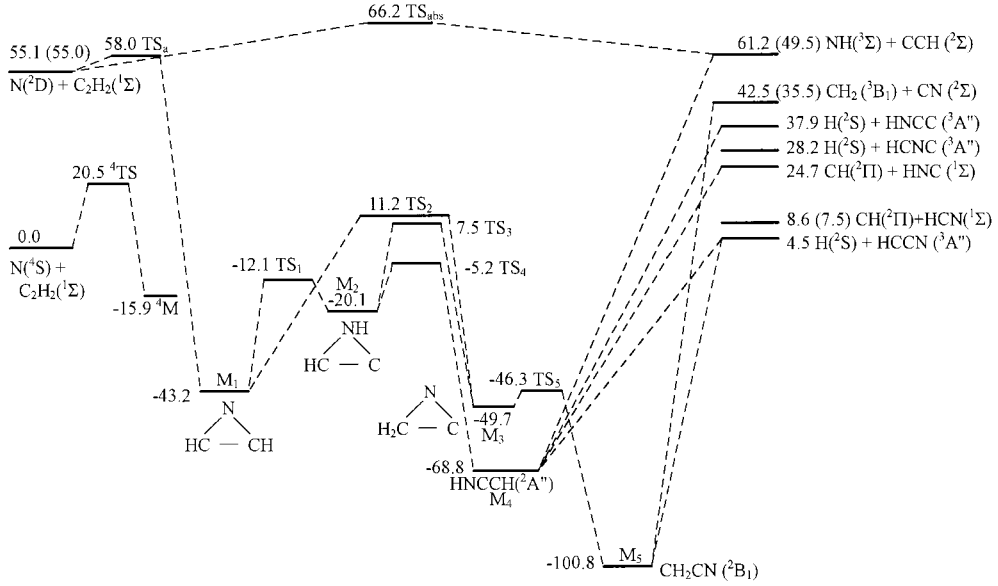

Figure 5. Calculated schematic energy diagram (units in kcal/mol) for the N + C_2H_2 reaction at the PMP4(full,SDTQ)/cc-pVTZ level. Values in parentheses are corresponding experimental data taken from ref 19. The energy level of N(^{4}S) + C_2H_2 is set to be zero.

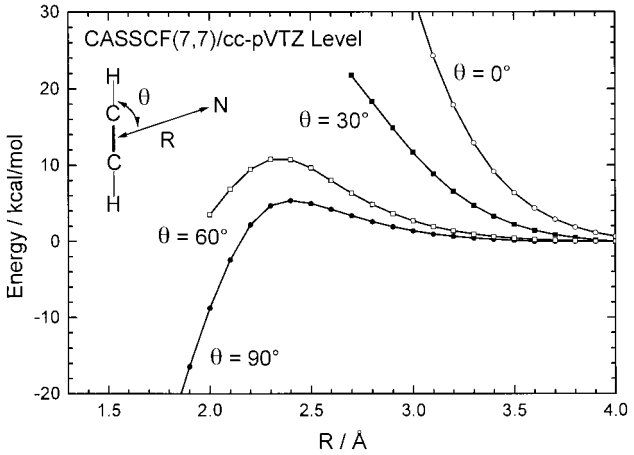

Figure 6. Potential energy curves as functions of the distance between N(^{2}D) and the midpoint of CC and the orientation angle calculated at the CASSCF(7,7)/cc-pVTZ level.

To obtain the information on the reactivity of N(^{4}S), we have also calculated the transition-state structure for the N(^{4}S) + C_2H_2 reaction. Figure 7 shows the molecular geometries for the transition state (denoted as ^{4}TS) of the addition of N(^{4}S) to C_2H_2 and for the subsequent intermediate complex (denoted as ^{4}M). The geometries were optimized at the MP2/cc-pVTZ level of theory. In contrast to the N(^{2}D) case, the N(^{4}S) atom primarily adds to one of the carbon atoms of C_2H_2. The energy diagram for the addition of N(^{4}S) to C_2H_2 is schematically shown in Figure 5. The barrier height including zero-point vibrational energy correction was calculated to be 20.5 kcal/mol at the PMP4(full,SDTQ)/cc-pVTZ level of theory. This result is qualitatively consistent with the fact that the measured rate constant for N(^{4}S) + C_2H_2 is extremely small[7,8] ($\sim 10^{-16}$ cm^3 molecule^{-1} s^{-1}).

C. Comparison of Theoretical and Experimental Rate Constants. The rate constants for the N(^{2}D) + C_2H_2 (C_2D_2) reaction have been calculated by conventional transition-state theory using the following usual equation.

$$k(T) = \frac{k_B T}{h} \frac{Q^{\ddagger}}{Q^{\mathrm{react}}} e^{-E_0/k_B T}$$

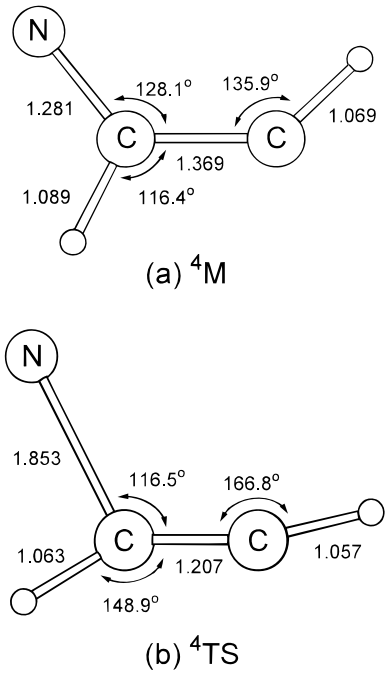

Figure 7. Molecular geometries of the stationary points on the potential energy surface of the N(^{4}S) + C_2H_2 reaction: (a) ^{4}M and (b) ^{4}TS.

The partition functions for the reactants (Q^{react}) as well as the transition state ($Q^{\ddagger}$) were calculated using the ab initio vibrational frequencies and moments of inertia, which were obtained at the CASSCF(7,7)/cc-pVTZ level of theory. Note that the partition function should include the contribution of electronic states as $Q = Q_{\mathrm{el}}Q_{\mathrm{trans}}Q_{\mathrm{vib}}Q_{\mathrm{rot}}$. If we assume that only the lowest doublet potential energy surface is reactive, the ratio of the electronic partition functions between the reactant and the transition state, $Q^{\ddagger}_{\mathrm{el}}/Q^{\mathrm{react}}_{\mathrm{el}}$ becomes 1/5, because the electronic state of N(^{2}D) is 5-fold degenerate (without spin−orbit interaction). In addition, we employ the ab initio barrier height of 2.9 kcal/mol calculated at the PMP4(full,SDTQ)/cc-pVTZ level of theory. The rate constants thus calculated are compared to the experimental rate constants in Figure 8. It is seen that the calculated rate constants are much smaller than

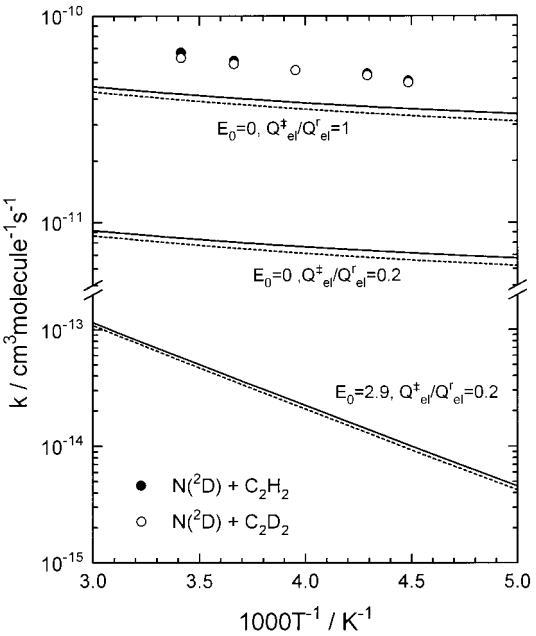

Figure 8. Arrhenius plots of the rate constants for the N(^{2}D) + C_2H_2 and C_2D_2 reactions. Lines represent the rate constants calculated by conventional transition-state theory with three different parameters (see text). Filled and open circles correspond to the present experimental data.

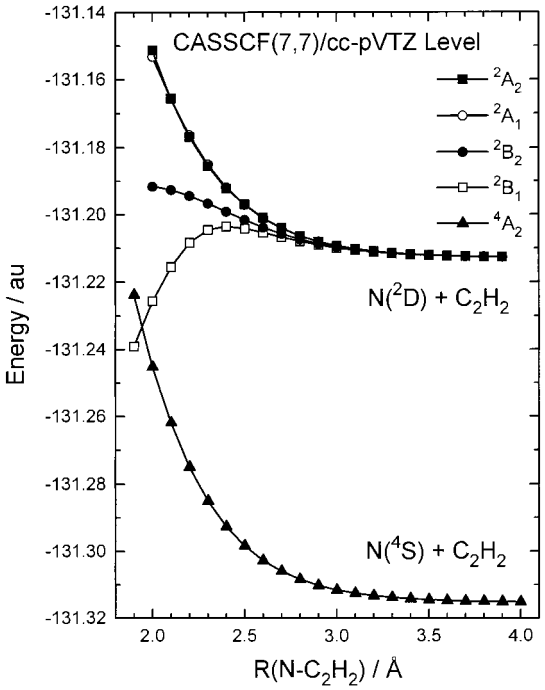

Figure 9. Total electronic energies as a function of the distance between N and the midpoint of CC for the lowest four doublet states and one quartet state calculated at the CASSCF(7,7)/cc-pVTZ level.

the experimental ones by a factor of 10^3-10^4. This serious disagreement primarily is attributed to the inaccuracy in the ab initio barrier height since it is generally accepted that a highly correlated method with a large basis set is required to obtain a more accurate barrier height. Therefore, we reduced the barrier height to 0 kcal/mol and compared to the experimental data. The result is also plotted in Figure 8. It has been found that the calculated rate constants are still smaller than the experimental ones by a factor of about 7. The inclusion of quantum-mechanical tunneling generally enhances the rate constant. We have estimated the contribution of tunneling with a simple Wigner approximation. As a result, we found that tunneling can safely be ignored. This is also understandable since the tunneling motion is associated with the relative translational motion between N and C_2H_2, in which the corresponding reduced mass is relatively large. The results of these calculations strongly suggest that we have to consider other reasons except for the inaccuracy in the barrier height.

First, we discuss the contribution of electronically excited states since there should exist five doublet potential energy surfaces which asymptotically correlate to N(^{2}D) + C_2H_2 without spin−orbit interaction. To discuss this point, we calculated the potential energies for the lowest four states which asymptotically correlate to N(^{2}D) + C_2H_2. The calculations were carried out at the CASSCF(7,7)/cc-pVTZ level of theory within C_{2v} symmetry. Figure 9 displays the total energies as a function of R, which is the distance between N and the midpoint of CC. The geometry of C_2H_2 was kept in the reactant geometry. It can easily be seen that only the lowest $^2B_1$ state is reactive with a small barrier height; however, these four states are very close in energy for $R > 2.5$ Å. If we assume that the rate constants for mixing (nonadiabatic transition) among the five states are much larger than the addition rate constant, the ratio of the electronic partition functions between the reactant and transition state, $Q^‡_{el}/Q^{react}_{el}$ approximately becomes unity. This simply increases the calculated rate constants by a factor of 5, and the result is plotted in Figure 8. The agreement with the experimental data is seen to be better although the calculated rate constants are slightly smaller than the experimental data. It should be emphasized, however, that the validity of this assumption is unclear.

Next, we discuss the possibility of the quenching process, N(^{2}D) + C_2H_2 → N(^{4}S) + C_2H_2. We calculated the potential energy curve for the quartet state which asymptotically correlates to N(^{4}S) + C_2H_2 at the CASSCF(7,7)/cc-pVTZ level under C_{2v} symmetry. The curve is also displayed in Figure 9. The result in Figure 9 qualitatively suggests that the quenching process may be less important because there are no crossing points before N(^{2}D) + C_2H_2 reaches the transition state. It is seen that the potential curves for the $^4A_2$ and $^2B_1$ states cross at around $R = 2$ Å. This tentatively suggests the existence of the intersystem crossing process from the lowest doublet surface to the quartet surface. The reaction rate for this process, however, should be determined by the transition state TS_a.

Finally, we discuss approximations employed in the present transition-state theory calculations: neglect of vibrational anharmonicity and variational effect. The most important anharmonic effect comes from the low-frequency vibrational mode at the saddle point (162 cm^{-1}, see Table 3). This mode mainly corresponds to the in-plane bending motion of the N atom with respect to the C_2H_2 molecule and asymptotically correlates to the free rotation. It is generally known that the inclusion of anharmonicity in the bending mode increases the vibrational energy levels in the transition state and hence decreases the calculated rate constants. Therefore, the inclusion of anharmonicity would exacerbate the discrepancy between theory and experiment. We have also ignored so-called "variational effect", which can be estimated by locating the dynamical bottleneck. The variational effect would probably be important because the barrier height for the N(^{2}D) + C_2H_2 reaction is very low. However, to discuss this effect quantitatively, a global potential energy surface and/or a vibrational analysis along the reaction coordinate at higher levels of theory will be needed. Such a calculation is currently beyond our computational capability.

5. Conclusions

The rate constants for the reactions $N(^2D) + C_2H_2(C_2D_2)$ and $N(^2P) + C_2H_2(C_2D_2)$ have been measured using a pulse radiolysis−resonance absorption technique at the temperature range between 223 and 293 K. Arrhenius parameters of the rate constants for these reactions have been reported. The H/D isotope effect has been found to be very small for both the $N(^2D)$ and $N(^2P)$ reactions. The absolute values of the rate constants for $N(^2D) + C_2H_2$ were about 3 times as large as those for $N(^2P) + C_2H_2$. This result is in high contrast to the case of saturated hydrocarbon molecules, suggesting the deactivation mechanisms of $N(^2P)$ by C_2H_2 are different from those by saturated hydrocarbons. Ab initio molecular orbital calculations have been carried out for the lowest doublet potential energy surface of the $N(^2D) + C_2H_2$ reaction in order to understand the reaction mechanisms and the possible reaction pathways. It has been found that the initial step of this reaction is the addition of $N(^2D)$ to the π-bond of C_2H_2. The rate constants for the $N(^2D) + C_2H_2$ reaction have been calculated by transition-state theory using the ab initio results and compared to the experimental results. The serious disagreement has been found even if we consider the inaccuracy in the ab initio barrier height. This result strongly suggests that the information on the mixing processes (nonadiabatic transitions) among five potential energy surfaces will be required for further qualitative discussion and that the contribution of the variational effect should qualitatively be studied. Nevertheless, the present ab initio molecular orbital results should provide a useful starting point for calculations at higher levels of theory.

Acknowledgment. T.T. is grateful to Professor P. Casavecchia for many informative conversations and e-mail communications.

References and Notes

(1) Safrany, D. R. *Prog. React. Kinet*. **1971**, *6*, 1.

(2) Umemoto, H.; Kimura, Y.; Asai, T. *Chem. Phys. Lett*. **1997**, *264*, 215.

(3) Umemoto, H.; Kimura, Y.; Asai, T. *Bull. Chem. Soc. Jpn*. **1997**, *70*, 2951.

(4) Gonzalez, C.; Schlegel, H. B. *J. Am. Chem. Soc*. **1992**, *114*, 9118.

(5) Kurosaki, Y.; Takayanagi, T.; Sato, K.; Tsunashima, S. *J. Phys. Chem*. **1998**, *102*, 254.

(6) Safrany, D. R.; Jaster, W. *J. Phys. Chem*. **1968**, *72*, 3305.

(7) Avramenko, L. I.; Krasnen'kov, V. M. *Izv. Akad. Nauk SSSR, Ser. Khim*. **1964**, *5*, 822.

(8) Umemoto, H.; Nakagawa, S.; Tsunashima, S.; Sato, S. *Bull. Chem. Soc. Jpn*. **1986**, *59*, 1449.

(9) Fell, B.; Rivas, I. V.; McFadden, D. L. *J. Phys. Chem*. **1981**, *85*, 224.

(10) Umemoto, H.; Sugiyama, K.; Tsunashima, S.; Sato, S. *Bull. Chem. Soc. Jpn*. **1985**, *58*, 3076.

(11) Alagia, M.; Balucani, L.; Catechini, P.; Casavecchia, P.; van Kleef, E. H.; Volpi, G. G. Private communication.

(12) Suzuki, T.; Shihira, Y.; Sato, T.; Umemoto, H.; Tsunashima, S. *J. Chem. Soc., Faraday Trans*. **1993**, *89*, 995.

(13) Frisch, M. J.; Trucks, G. W.; Schlegel, H. B.; Gill, P. M. W.; Johnson, B. G.; Robb, M. A.; Cheeseman, J. R.; Keith, T.; Petersson, G. A.; Montgomery, J. A.; Raghavachari, K.; Al-Laham, M. A.; Zakrzewski, V. G.; Ortiz, J. V.; Foresman, J. B.; Cioslowski, J.; Stefanov, B. B.; Nanayakkara, A.; Challacombe, M. C.; Peng, Y.; Ayala, P. Y.; Chen, W.; Wong, M. W.; Andres, J. L.; Replogle, E. S.; Gomperts, R.; Martin, R. L.; Fox, D. J.; Binkley, J. S.; Defrees, D. J.; Baker, J.; Stewart, J. P.; Head-Gordon, M.; Gonzalez, C.; Pople, J. A. *Gaussian 94*; Gaussian, Inc.: Pittsburgh, PA, 1995.

(14) Dunning, T. H., Jr. *J. Chem. Phys*. **1989**, *90*, 1007.

(15) Bowman, C. R.; Miller, W. D. *J. Chem. Phys*. **1965**, *42*, 681.

(16) (a) Wetmore, R. W.; Schaefer, H. F., III. *J. Chem. Phys*. **1978**, *69*, 1648. (b) Yamaguchi, Y.; Vacek, G.; Schaefer, H. F., III. *Theor. Chim. Acta* **1986**, *86*, 97.

(17) Lischka, H.; Karpfen, A. *Chem. Phys*. **1986**, *102*, 77.

(18) Bowman, J. M.; Gazdy, B.; Bentley, J. A.; Lee, T. J.; Dateo, C. E. *J. Chem. Phys*. **1993**, *99*, 308.

(19) *JANAF Thermochemical Tables*, 3rd ed.; Natl. Stand. Ref. Data Ser. (U.S., Natl. Bur. Stand.); U.S. GPO: Washington, DC, 1985.

(20) Dendramis, A.; Lero, G. E. *J. Chem. Phys*. **1977**, *66*, 4334.